ISSN 2176-5480

22nd International Congress of Mechanical Engineering (COBEM 2013)
November 3-7, 2013, Ribeirão Preto, SP, Brazil

MORPHING AIRFOIL: CAMBER OPTIMIZATION USING SHAPE MEMORY ALLOYS

Lafaete Creomar Lima Junior
Marcelo A. Savi
Universidade Federal do Rio de Janeiro
COPPE – Department of Mechanical Engineering
21945-970 – Rio de Janeiro – RJ - Brazil
lclj@poli.ufrj.br, savi@mecanica.ufrj.br

Darren J. Hartl
Dimitris C. Lagoudas
Texas A&M University
Department of Aerospace Engineering
TX 77843 – College Station – USA
darren.hartl@tamu.edu, lagoudas@tamu.edu

Abstract. *Shape memory alloy (SMA) suffers phase transformations due to temperature or stress variations, responding to these variations in much more intense way than other materials. This characteristic and the large energy density of these transformations lead these materials to be used as actuators on certain applications, especially those where the transformation velocity is not a critical factor. Besides, the aerospace engineering looks forward to find solution that improves the lift capabilities of a wing without the conventional mechanical actuators, gaps and hinged surfaces. One of the possible solutions is to use SMAs on the wing structure in order to allow it to change its shape, mostly changing the camber, improving the lift for take offs and landings and returning to the original shape during the cruise flight. The characteristics of the SMA inserts are optimized combining the finite element analysis, which defines the deformed shape of a given configuration, the panel method, which defines the aerodynamic performance of the resultant shape, and the gradient method, combining these results, evaluating them and seeking better configurations until a local minimum is reached. After a reasonable number of runs, one can define the best result among these local minima as the best configuration in a given domain.*

Keywords: *Shape memory alloy, gradient, airfoil, finite element, optimization.*

1. INTRODUCTION

Aerospace applications have several challenges. The airfoil profile selection is an important one since the airfoil is designed for one flight situation and ancillary accessories are designed to cover the others. These accessories add complexity, weight and reduce the overall airplane wing reliability and efficiency. Besides, they also add discontinuities, becoming a source of noise and vibration.

This paper describes the development of an alternative solution, morphing airfoil and wing. This is not a new concept; morphing airfoils and wings have been used before in order to change the wingspan, the chord and other wing characteristics. These previous devices were commonly based on complex mechanical systems, having the same problems related on the previous generation described (Sofla *et al.*, 2009).

Shape memory alloys (SMAs) belong to the class of smart materials and offer an alternative solution for morphing wings, reducing the mechanical complexity of the mechanisms. They can be placed on the airfoil structure, eliminating the discontinuities and costing less in terms of weight than the traditional solutions.

The main goal of this contribution is to find the best geometries to a case study, attending two different flight situations. Finite element analysis is employed to investigate the system behavior. Panel method and gradient method are employed to evaluate flight conditions.

2. CASE STUDY

The airfoil investigated is related to a case study of a long-range heavy bomber, the Boeing B-29 Superfortress. This kind of airplane requires a high payload capacity and high flying efficiency in order to improve the flight range. However, the final airfoil selection shall compromise these two requirements. Table 1 shows the airplane specifications that lead the following analysis (Boeing).

ISSN 2176-5480

Table 1: Boeing B-29 technical specifications.

Length	30,18 m
Wing span	43,06 m
Height	8,5 m
Wing plain area	161,3 m²
Aspect Ratio	11,5
Empty weight	33.800 kg
Takeoff weight	54.000 kg
Maximum takeoff weight	60.650 kg
Power	4×1.640 kW
Maximum speed	574 km/h
Cruise speed	350 km/h
Stall speed	170 km/h
Flight range	5.230 km
Flying ceiling	9.710 m

Table 2 shows the two different flight situations contemplated by this study: the takeoff and the cruise flight (Incropera *et al.*, 2008). The takeoff condition requires the highest lift coefficient possible while the cruise flight requires the smallest drag possible. Therefore, there is always a compromise, because an airplane with an airfoil with huge lift coefficient and huge drag coefficient does not have enough power to reach the correct flight speed, besides, higher drag forces implies on higher power demand, resulting in higher fuel consumption, for instance.

Table 2: evaluated flight conditions.

Properties	Takeoff	Cruise flight
Altitude	0 m	7283 m
Speed	56,7 m/s	94,4 m/s
Specific Mass	1,225 kg/m³	0,5714 kg/m³
Dynamic viscosity	17,894 μPas	15,516 μPas
Kinematic viscosity	14,61 m²/s	27,17 m²/s
Pressure	101325 Pa	39520 Pa
Sound speed	340 m/s	311 m/s
Reynolds	15,5×106	13,9×106
Mach	0,17	0,30

In order to simplify the airfoil selection, this study is restricted to the NACA 4 digit series. These airfoils are used on many aerodynamics studies for years, resulting on a broad database available (Marzocca, 2004.). The main geometry change proposed herein is to produce an increased camber for the takeoff, reproducing the effect of the flaps and a reduced camber on the cruise flight.

The cruise flight airfoil selected is the NACA 4415 and as a first evaluation of this paper idea, the takeoff airfoil is the NACA 8415. Using the flight conditions previously defined, one can plot the takeoff polar, as shown in Figure 1. At this situation the airfoil with the higher camber, NACA 8415, has higher lift coefficients on the low drag area, being more adequate to the takeoff condition than the lower camber airfoil, NACA 4415.

ISSN 2176-5480

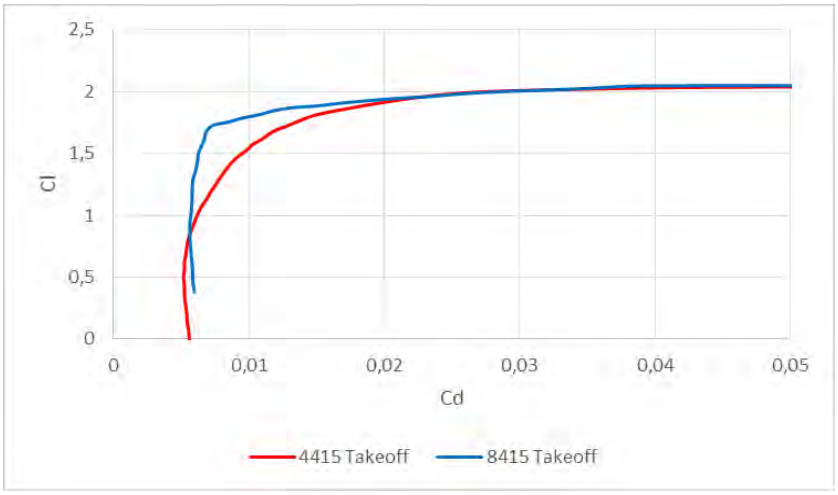

Figure 1: NACA 4415 x NACA 8415 Cl x Cd takeoff polar.

Following the same methodology, one can plot the cruise flight polar, as shown in Figure 2. When at lower lift coefficients, below 1.2, the lower camber airfoil has smaller drag coefficients, representing a better option on the cruise flights.

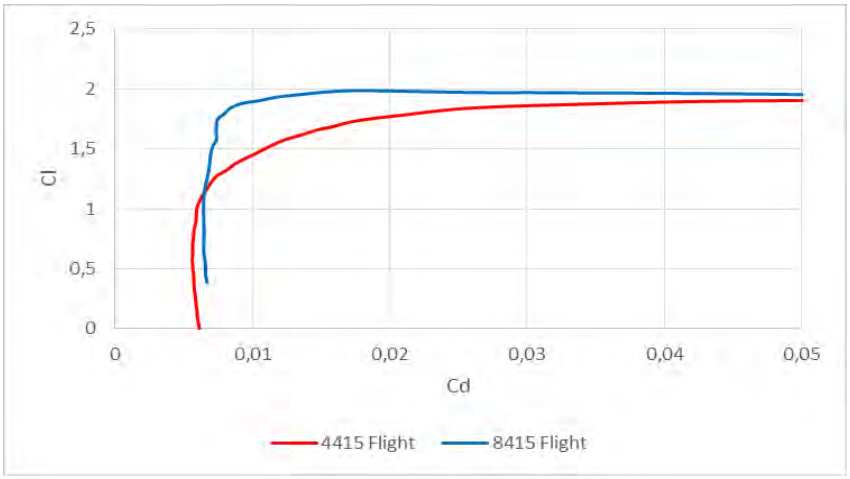

Figure 2: NACA 4415 x NACA 8415 Cl x Cd cruise flight polar.

The ideal airfoil selection would have the following aerodynamic performance, as shown in Figure 3. The airfoil geometry on takeoff will be closer to NACA 8415, with higher lift coefficients and the cruise flight would be on NACA 4415 with lowest drag coefficient for low lift coefficients. Figure 4 shows this concept.

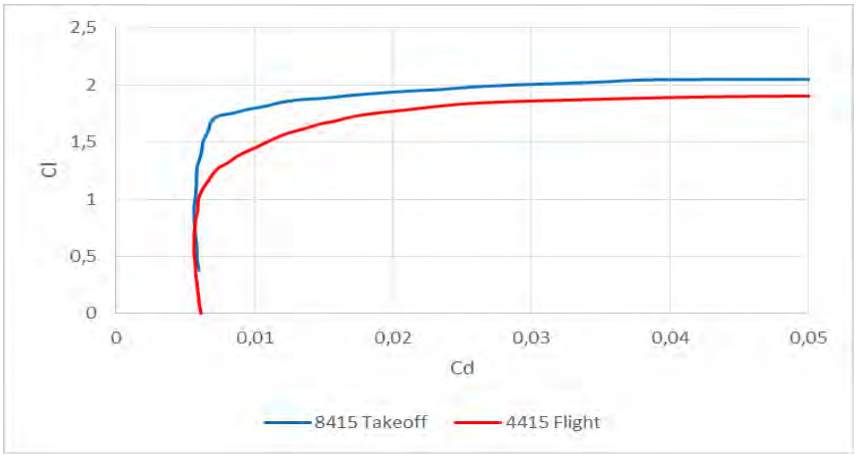

Figure 3: Morphing airfoil Cl x Cd polar.

ISSN 2176-5480

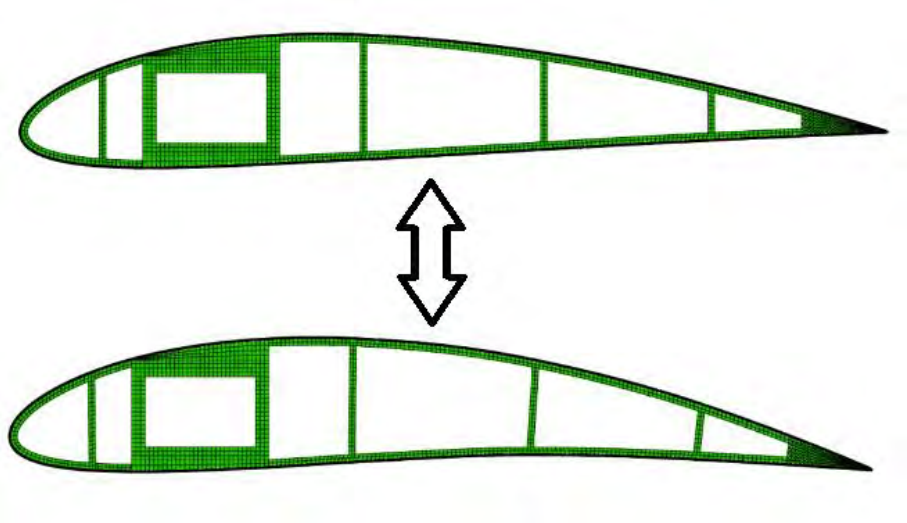

Figure 4: Conceptual representation of the camber change.

3. SHAPE MEMORY ALLOYS

The interest on the shape memory alloys relies on the phase transformation phenomenon. The nickel-titanium alloys present two distinct phases, martensitic, found at low temperatures, with higher flexibility, which can be found as twinned and de-twinned variants; and austenitic phase, found at higher temperatures, with superior stiffness (Silva, 2005).

The phase change occurs both ways, but they are triggered at different temperatures. When a sample are at low temperature, maintaining the stress constant, and its temperature increases, the sample stays on martensitic phase until it reaches the austenitic start temperature, when the phase transformation is triggered, and goes until the temperature reaches the austenitic final, when the sample is completely austenitic (Hartl and Lagoudas, 2007; Lagoudas, 2008). The opposite phase transformation is similar, but at different temperatures. Figure 5 shows the schematic picture of this behavior.

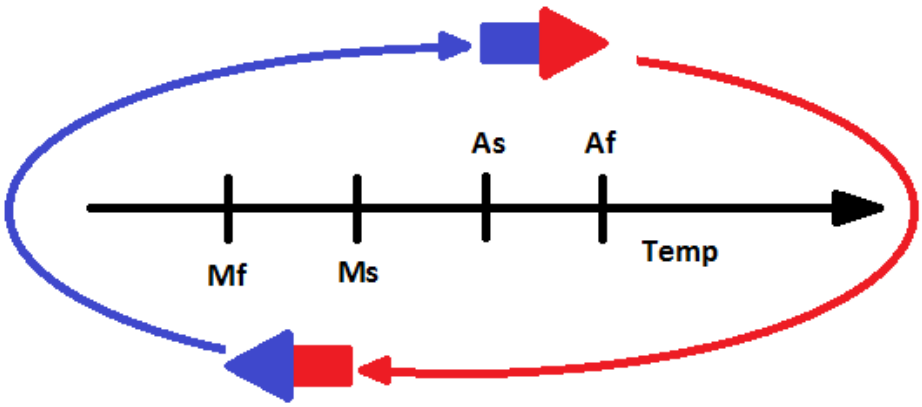

Figure 5: SMA behavior

Phase transformations change the material properties as Young modulus, yield and ultimate tensile strength; however, this study focuses on the strain capabilities of this transformation. When properly trained, Ni-Ti alloy reaches 8% strains, a value much higher than the thermal strain to the same temperature variation.

The addition of copper on these alloys increases the fatigue resistance, the response speed and the damping capability; it also reduces the temperature hysteresis and the temperature sensitivity due to the composition. NiTiCu alloys are also more predictable than NiTi alloys (Li et al., 2005; Jones and Dye, 2013). These characteristics are highly desirable on actuators, which also benefits on the high energy density of these phase transformations.

The finite element method is employed to investigate the initial and final states of the SMA. It also considers the SMA pieces fully trained with homogeneous properties along the part; the strain model is a temperature strain due to a temperature unitary step. Martensitic and austenitic different mechanical properties are considered.

ISSN 2176-5480

4. AERODYNAMIC PERFORMANCE

In order to characterize the aerodynamic performance, dimensionless coefficients are employed. The lift coefficient, drag coefficient and glide ratio are used herein.

The lift coefficient is the dimensionless value represented by the lift force of the airfoil at specific flight conditions, per medium specific mass, squared speed and chord (Abbott, 1950; Ruijgrok, 2009):

$$C_l = 2l/(\rho V^2 c) \quad (1)$$

The same can be done on the drag coefficient (Abbott, 1950; Ruijgrok, 2009):

$$C_d = 2d/(\rho V^2 c) \quad (2)$$

The glide ratio is the lift coefficient divided by the drag coefficient. This ratio is also dimensionless.

For the sake of simplicity, a two-dimensional panel method is employed instead of the complex three-dimensional evaluation using computer fluid dynamics. The first step for the application of this method is to divide the outer surface of the airfoil in panels (Oueslati *et al.*, 2005). Plane panels are employed, followed by the calculation of the tangential velocities on each panel (Manson, 1998). Since this case study has Mach number smaller than 0.3, the flow is considered incompressible and the pressure can be evaluated using Bernoulli (Fox and McDonald, 1981). Once the pressure is known, it can be integrated through the whole airfoil and decomposed on the lift and drag components.

This study uses 100 panels for the discretization, as showed in Figure 6. The use of more panels changes just slightly results (Mason, 1998; Oueslati *et al.*, 2005).

The panel method does not have the reliability to predict the drag forces on real application; however, as this study kept the same number of panels and same boundary conditions, these results can be used to identify the trends and, later on, used to find the smallest drags on the studied airfoils.

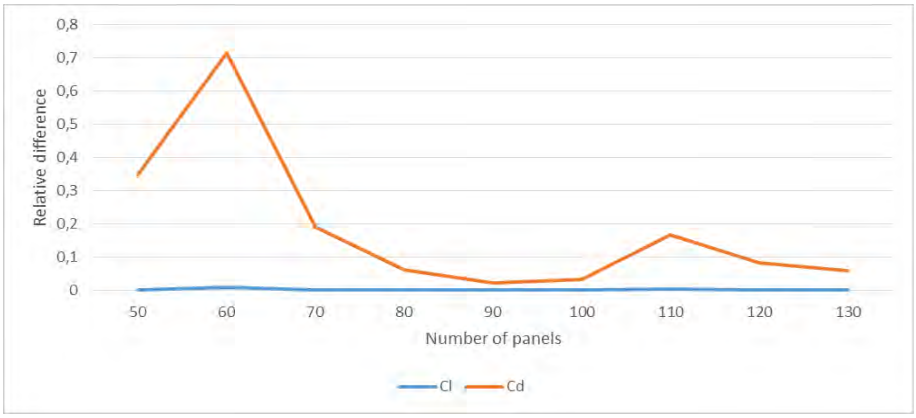

Figure 6: Number of panels' analysis.

5. WING GEOMETRY

The finite element method is employed for the wing analysis. A two-dimensional model is employed to represent the three-dimensional wing as an infinite span wing (Abbot, 1950). Under this assumption, the flow phenomenon is evaluated to the effects that can be described on the chord plane. This simplification evaluates effects neither described on spar plane nor complex three-dimensional effects. Figure 7 shows the employed model.

ISSN 2176-5480

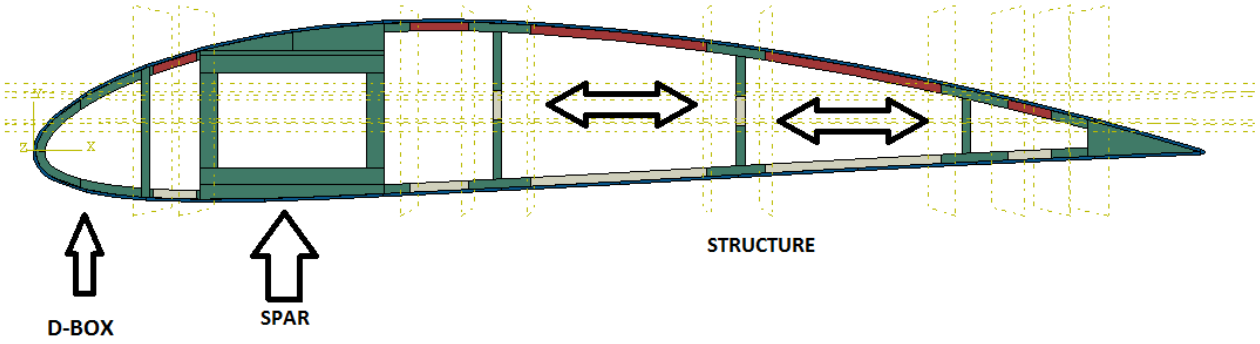

Figure 7: Proposed geometry.

A box spar gives the wing the necessary stiffness, both flexural and torsional. It also transfers the flight loads from the wings to the airplane fuselage. The box geometry results in a spar with larger inertia moment than a similar mass, full beam, maximizing the compromise weight versus functionality. The D-box is a secondary spar that, besides the wing stiffness function, also guarantees the preservation of the leading edge geometry, once this airfoil portion suffers the highest flying loads and is the most sensitive airfoil portion to shape change. These two devices go through the whole wingspan. These two structures are made in aluminum, the green material on Figure 7, which mechanical properties are presented in Table 3 (Callister Jr, 2008; Budynas and Nisbett, 2011; Norton 2004). Another wing feature is the internal profile structure, responsible to transfer the flight loads from the wing skin to the spars and hold the SMA inserts into the designed position.

Table 3: Aluminum mechanical properties.

Aluminum 7075 T6	
Young modulus	71,7 GPa
Poisson coefficient	0,33
Yield strength	503 MPa
Ultimate tensile strength	572 MPa

The wing has a polymeric skin responsible to conduct the flow and allow the shape change. As it is supported by the airfoil structure, the main requirement for this feature is to resist the SMA actuators strain, the Tecoflex 80-A fits for this purpose, represented by the blue color skin in Figure 7. Table 4 shows its mechanical properties (Kikuta, 2003).

Table 4: Tecoflex 80-A mechanical properties.

Tecoflex 80-A	
Young modulus	71 kPa
Maximum strain	30%

The red and the gray features in Figure **7** represent the twelve SMA inserts. All the red inserts will suffer the martensitic-austenitic phase transformation while the gray ones will go through the austenitic-martensitic phase transformation, and vice-versa. In other words, these groups have antagonistic phase transfomation. Since phase transformations occur, the SMA strain modifies the whole airfoil geometry, increasing or decreasing the camber. Table 5 shows the SMA properties employed (Shape Memory Applications, Inc, 1999).

ISSN 2176-5480

Table 5: SMA mechanical properties.

SMA TiNiCu	
Strain	4%
Martensitic	
Young modulus	40 GPa
Poisson coefficient	0,3
Yield strength	500 MPa
Ultimate tensile strength	895 MPa
Austenitic	
Young modulus	83 GPa
Poisson coefficient	0,3
Yield strength	130 MPa
Ultimate tensile strength	895 MPa

The following insert denomination is adopted to describe the result, the upper surface names start with S and the lower surface names start with I, followed by its number, counted from leading edge to trailing edge. The internal inserts have the letter E and their number. For example, the insert named I2 is the second lower insert. Figure 8 shows the schematic representation.

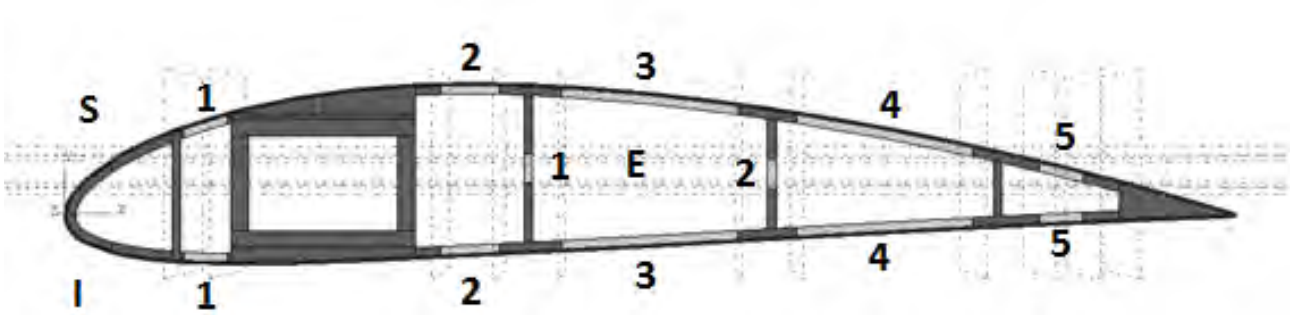

Figure 8: SMA insert names.

6. OPTIMIZATION ALGORITHM

An optimization algorithm is employed to evaluate the SMA positions. The optimized variable is the length of the inserts. The number and the position of the center are fixed, together with the mechanical properties. It begins with the shotgun method that creates multiple random start points; an optimization run begins on each of them, increasing the reliability of the minimum found. Bigger number of starting points means more paths evaluated, increasing the probability of the local minimum found to be the smallest minimum on the domain.

After the definition of the pivot, the next step is to create the neighbors, points with a small offset on one direction from the pivot, used to estimate the gradient at the pivot. These points represent different configurations of the airfoil; a finite element software evaluates each of them and exports the resulting shape back into the algorithm.

The algorithm allows two different approaches: a shape comparison; and the aerodynamic performance comparison. Here, the second approach is of concern. The shapes imported from the finite element analysis are then, repositioned, in order to avoid inaccurate results due to and attack angle not taken into account. Then a panel method analysis returns the lift and drag coefficients of each simulated geometry. The algorithm evaluates the stop criterion: if true, this is a result; if false, these values generate the gradient, which defines the next pivot by subtracting the gradient times a pitch, *p*, here a fixed scalar value (Shewchuk, 1994; Aziri, 2007; Ruggiero and Lopes, 1996). Figure 9 presents a schematic representation of the algorithm.

$$\{\text{next pivot}\}=\{\text{pivot}\}-p*\{\text{gradient}\} \quad (3)$$

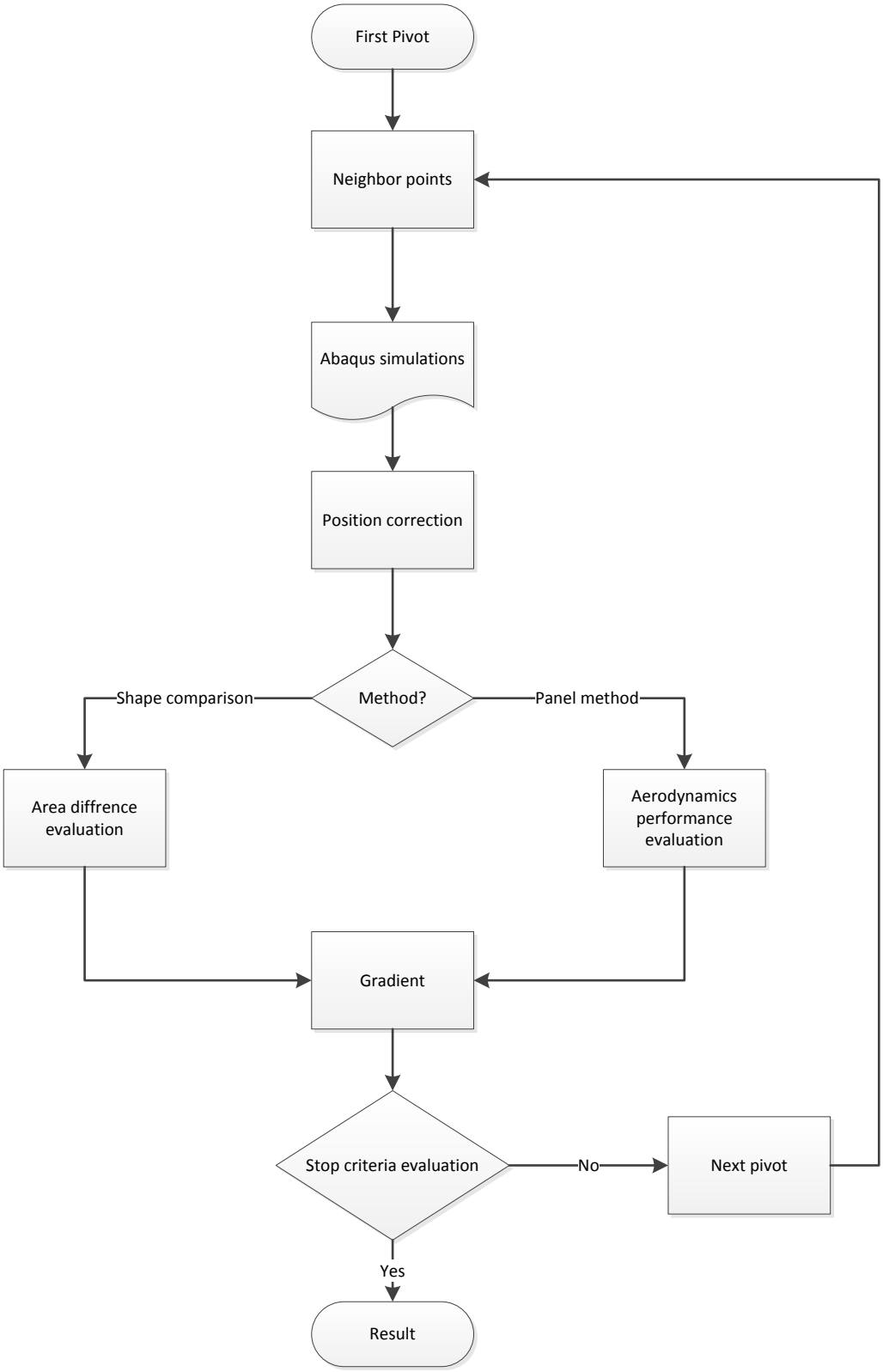

Figure 9: Optimization algorithm.

7. RESULTS

This section presents results related to the numerical simulations. The idea is to show results showing the different aerodynamic performance related wing configurations, altered by SMA actuators. Table 6 shows the largest glide ratio result, 179 larger than the glide ratio of the start airfoil, NACA 4415, 166, as expected.

ISSN 2176-5480

Table 6: Result.

Insert	Length	Insert	Length	Insert	Length
S1	20,56 mm	S2	142,76 mm	S3	478,77 mm
S4	271,06 mm	S5	5,0 mm	I1	150,0 mm
I2	65,77 mm	I3	415,64 mm	I4	178,5 mm
I5	5,0 mm	E1	154,22 mm	E2	301,51 mm
Cl/Cd max			179		

Figure 10 shows the aerodynamic performance of some configurations. The resulting airfoil has larger lift coefficient, but this only occurs at high drag ratios, which can be plausible on takeoff situation where the low speed does not demand more power than available. On the low lift and low drag coefficients, the difference between the airfoil performances is imperceptible, but the resulting airfoil have smaller drag for the same lift in this area.

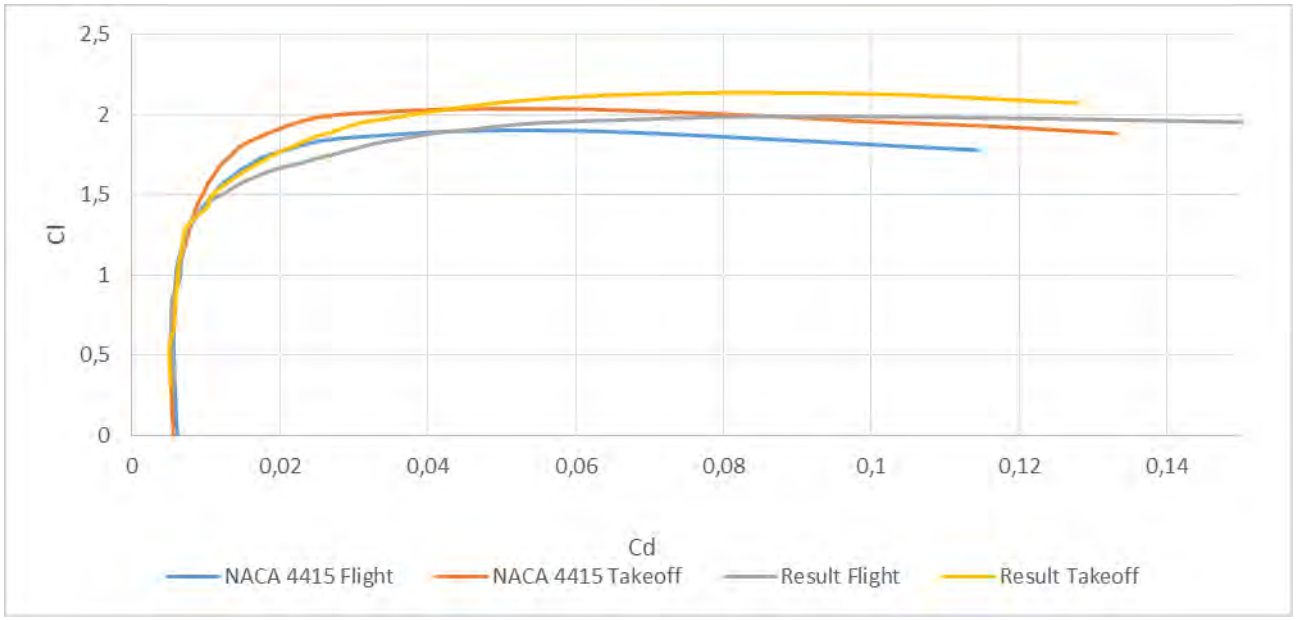

Figure 10: NACA 4415 and resulting airfoil Cl x Cd polar.

Figure 11 shows the glide ratio. The resulting airfoil curve is dislocated to the left, which results on the same glide ratio value on smaller attack angles. This can be interesting; the wing can be installed on an optimum position for the cruise flight and, as it is actuated to the takeoff situation, this phenomenon compensates the smaller installation angle.

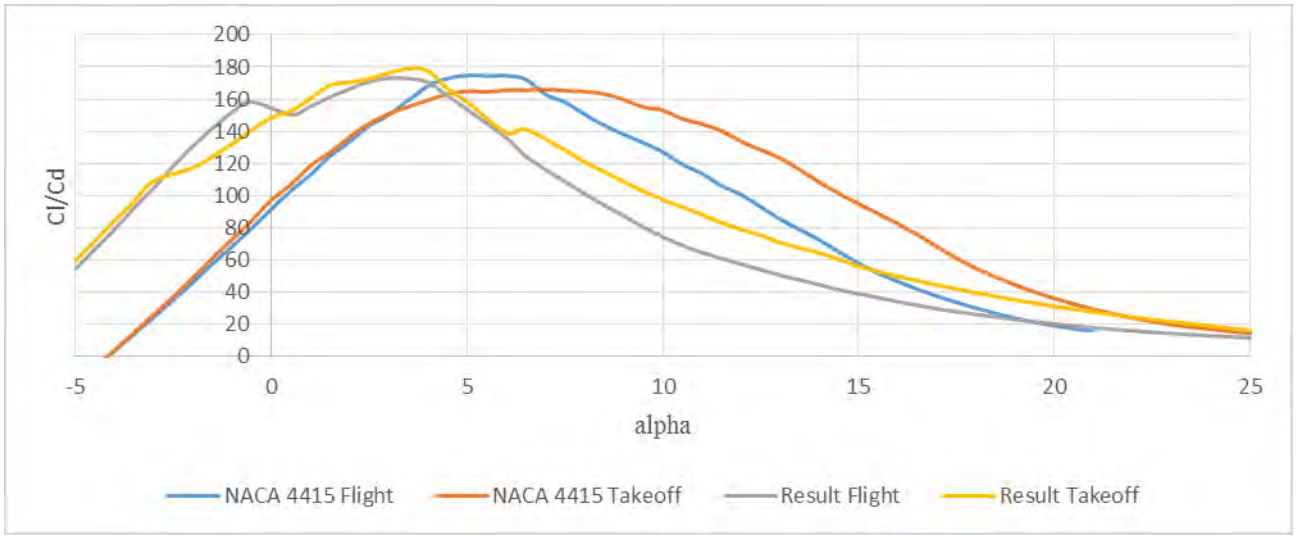

Figure 11: NACA 4415 and resulting airfoil glide ratio.

ISSN 2176-5480

8. CONCLUSIONS

This paper deals with the use of SMAs as actuators for morphing airfoil purpose. In general, results show that it is possible to change the aerodynamics performance using SMA actuators. Results show the differences between the actuated and the non-actuated shapes. There are several challenges for the application of this idea in real applications. A three-dimensional investigation is important in this way, evaluating some effects as the wing torsion due to SMA actuation. Besides, the thermal behavior of the whole structure shall be evaluated, heat sources as the turbines and the heat transfer by the metallic structure must be taken in account. The manufacturing of the SMA inserts and its mechanical properties and fatigue resistance is another important issue. Finally, some airplane components may be repositioned; many aircrafts have their fuel tanks on the wing, which would restrain the shape change.

9. ACKNOWLEDGEMENTS

The authors would like to acknowledge the support of the Brazilian Research Agencies CNPq, CAPES and FAPERJ and through the INCT-EIE (National Institute of Science and Technology – Smart Structures in Engineering) the CNPq and FAPEMIG. The Air Force Office of Scientific Research (AFOSR) is also acknowledged.

10. REFERENCES

A.Y. N. Sofla, S. A. Meguid, K. T. Tan and W. K. Yeo, “Shape morphing of aircraft wing: Status and challenges,” *Materials and Design,* pp. 1284-1292, setember, 12th 2009.

Boeing, “B-29 Superfortress,”. [Online]. Available at: http://www.boeing.com/boeing/history/boeing/b29.page. [Acess: december 12th 2012].

F. P. Incropera, D. P. Dewitt, T. L. Bergman and A. S. Lavine, “Fundamentos de Transferância de Calor e de Massa”, Rio de Janeiro, RJ, Brazil: LTC, 2008.

P. Marzocca, “The NACA Airfoil Series”, Clarkson University, 2004.

R. F. Silva, “Metais com Memória de Forma,” Universidade de Aveiro, november 9th 2005. [Online]. Available at: http://www2.cv.ua.pt/QUIMIMATER/Protocolos%20Experimentais/Unidade1/Seminario_Metais%20com%20Memoria%20de%20Forma.pdf. [Acess: december, 15th, 2012].

D. J. Hartl and D. C. Lagoudas, “Aerospace applications of shape memory alloys,” Journal of Aerospace Engineering, p. 16, april, 11th, 2007.

D. C. Lagoudas, Shape Memory Alloys: Modeling and Engineering Applications, College Station, TX, USA: Springer, 2008.

Y.-H. Li, L. J. Rong, Z.-T. Wang, G.-X. Qi and C.-Z. Wang, “Temperature Memory Effect of Ti50Ni30Cu20 (at%) alloy,” Journal of Alloy Compounds, pp. 112-115, september 1st 2005.

N. G. Jones and D. Dye, “Influence of applied stress on the transformation behaviour and martensite evolution of a Ti-Ni-Cu shape memory alloy,” Intermetallics, pp. 239-249, october, 9th 2013.

I. H. Abbott, “Theory of Wing Sections”, New York, EUA: Dover Pubications, 1950.

G. J. J. Ruijgrok, “Elements of Airplane Performance”, Delft: VSSD, 2009.

M. Oueslati, A. Dahmouni, M. B. Salah, F. Askri, C. Kerkeni and S. B. Nasrallah, “Aerodynamic Performances of Wind Turbine Airfoils Using a Panel Method,” Journal of Environmental Science and Engineering, pp. 1175-1182, 2005.

W. H. Mason, “Incompressible Potential Flow Using Panel Methods,” in Applyed Computational Aerodynamics, Blacksburg, Viginia Tech, 1998, pp. 4.1-4.68.

R. W. Fox and A. T. McDonald, “Introdução a Mecânica dos Fluidos”, Rio de Janeiro: Guanabara Dois, 1981.

W. D. Callister Jr., “Ciência e Engenharia de Materiais: Uma Introdução”, Rio de Janeiro, RJ, Brazil: LTC, 2008.

R. G. Budynas and J. K. Nisbett, “Elementos de Maquinas de Shigley: Projeto de Engenharia Mecânica”, Porto Alegre: AMGH Editora, 2011.

R. L. Norton, “Projeto de maquinas: Uma abordagem integrada”, Porto Alegre: Bookman, 2004.

M. T. Kikuta, “Mechanical Properties of Candidate Materials for Morphing Wings”, Blacksburg, 2003.

Shape Memory Applications, Inc., “Selected Properties of NiTi,” Shape Memory Applications, Inc., San Jose, 1999.

J. R. Shewchuk, “An Introduction to the Conjugate Gradient Method Without the Agonizing Pain”, Pittsburg, PA, 1994.

V. O. Aziri, “Conjugate Gradient Method”, Ames, 2007.

M. A. G. Ruggiero and V. L. d. R. Lopes, “Cálculo Numérico: Aspectos teóricos e computacionais”, São Paulo, SP, Brasil: Pearson Makron Books, 1996.

11. RESPONSIBILITY NOTICE

The authors are the only responsible for the printed material included in this paper.